EurJIC
European Journal of Inorganic Chemistry

Full Paper
doi.org/10.1002/ejic.202000387

Metallamacrocycles

Structural Versatility and Supramolecular Isomerism in Redox-Active Tetra- and Hexaruthenium Macrocycles

Daniel Fink,[a] Nicole Orth,[b] Michael Linseis,[a] Ivana Ivanović-Burmazović,[b] and Rainer F. Winter*[a]

Abstract: We report on six macrocyclic tetra- and hexaruthenium complexes formed by the self-assembly of 2,5-divinylthiophene- or 2,5-divinylfuran-bridged diruthenium and 2,5-thiophene-, -furan- or -pyrroledicarboxylate linkers. All complexes were scrutinized by NMR spectroscopy and UHR ESI-MS, cyclic and square wave voltammetry and, in five cases, by X-ray diffraction analyses. Although the utilized building blocks differ only slightly with respect to their intrinsic bite angles, the resulting macrocycles exhibit remarkable structural versatility. Electrolysis inside an optically transparent electrochemical (OTTLE) cell provided their associated di-/tri- and tetra-/hexacations, which were studied by IR, UV/Vis/NIR and EPR spectroscopy. The divinylthiophene-furandicarboxylate complex **2-TF** provides a rare example of supramolecular isomerism in metallamacrocyclic complexes. Thus, hexanuclear **2-TF$_6$** is initially formed as a kinetic isomer, which subsequently transforms slowly and cleanly into tetranuclear **2-TF$_4$**.

Introduction

Metallamacrocycles represent a fascinating class of cyclic molecules of intrinsic beauty due to their inherently high symmetry. They are generally constructed from transition metal-based nodes and appropriate polytopic organic linkers via self-assembly processes. Capitalizing on this highly modular synthetic approach, a vast array of metallamacrocyclic structures with various nuclearities and shapes have been realized since the pioneering work of Verkade.[1,2] Apart from their appealing beauty, metallamacrocycles are now entering practical applications as exemplified by ion sensing,[3] the selective binding of suitable guest molecules,[4] and their use as cytotoxic and anticancer agents,[5] or as Trojan horses for the delivery of $^1O_2$ sensitizers to cancer cells.[6] They may also act as tiny reaction vessels for studying chemical processes in confined spaces and environments.[7] Although most of these structures possess redox-active metal nodes or linkers, their electrochemical properties have long been neglected.[8]

Reports on the metal- or ligand-based redox activity of rectangular tetraplatinum, -rhenium, -ruthenium, -rhodium, and -iridium macrocycles can be found in the beautiful work of Hupp,[9] Therrien[10] and Sallé,[11] as well as that of Kaim and Stang.[12] Further examples are the investigations of ferrocene- or biferrocene-based macrocycles of Mayor[13] and Long[14] (for recent reviews on this topic see ref. 8). Other recent developments include the impressive work of Würthner on triruthenium macrocycles as the active species in photocatalytic water oxidation,[15] as well as the research of Sallé on the redox-controlled uptake or release of incorporated guest molecules.[16]

Our contribution to this field are investigations of macrocyclic complexes incorporating π-conjugated ruthenium vinyl entities and dicarboxylate linkers. In particular, we have reported on tetranuclear metallamacrocycles constructed from divinylphenylene-bridged diruthenium complexes and differently substituted isophthalic acid derivatives (Scheme 1, left). The resulting tetranuclear metallamacrocycles are oxidized reversibly to their respective di- and tetracationic forms. The latter absorb strongly in the visible (Vis) and in the near infrared (NIR), thus endowing these complexes with intriguing electrochromic properties.[17,18] By attaching additional redox-active moieties to the outer rim of the macrocycles, the reversible loss of up to eight electrons can be realized.[19] Tetraruthenium macrocycles of this architecture feature two π-conjugated metal-organic electrophores as the sides, which are mutually insulated from each other by the dicarboxylate linkers. As a consequence, such macrocycles undergo almost coincident oxidations of the individual sides to first their radical cationic and then their dicationic states, which give rise to two sets of overlapping one-electron responses in their cyclic or square-wave voltammograms.

This contrasts to the behavior of tri- and tetranuclear macrocycles made by self-assembly of the hydride complex HRu(CO)Cl(P^iPr_3)$_2$ with asymmetrically functionalized ethynylar-

[a] D. Fink, Dr. M. Linseis, Prof. Dr. R. F. Winter
Fachbereich Chemie, Universität Konstanz,
Universitätsstraße 10, 78457 Konstanz, Germany
E-mail: rainer.winter@uni-konstanz.de
[b] N. Orth, Prof. Dr. I. Ivanović-Burmazović
Department Chemie und Pharmazie, Friedrich-Alexander-Universität Erlangen-Nürnberg,
Egerlandstraße 1, 91058 Erlangen, Germany
Supporting information and ORCID(s) from the author(s) for this article are available on the WWW under https://doi.org/10.1002/ejic.202000387.

Full Paper
doi.org/10.1002/ejic.202000387

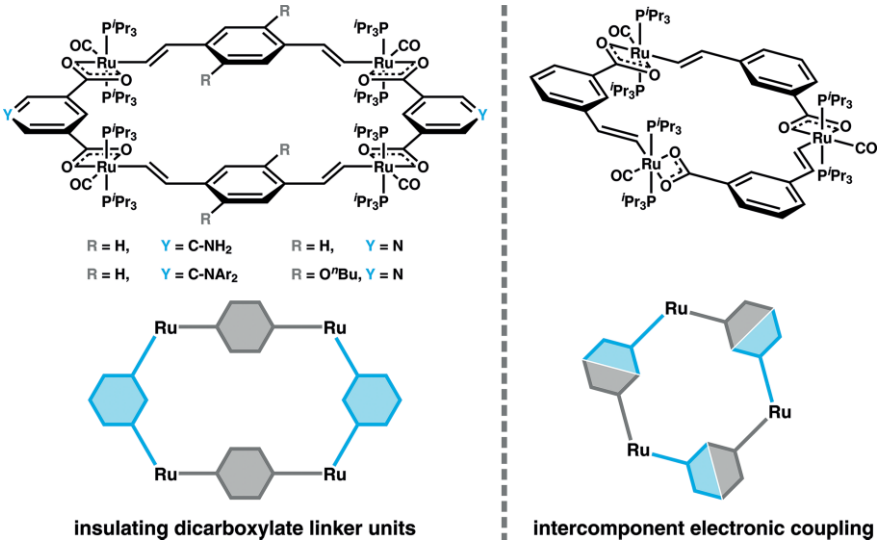

Scheme 1. Vinylruthenium based macrocyclic structures utilizing symmetric (left) or asymmetric building blocks (right) and corresponding graphical representations.[17,20]

ylcarboxylate linkers as self-complimentary building blocks (Scheme 1, right). Such systems were found to undergo three or four separate one-electron oxidations and to exhibit intracyclic through-bond charge delocalization in their mixed-valent states, thus representing rare examples of molecule-based conductive loops.[20,21]

The present study extends our previous work on the macrocyclic tetraruthenium complex **2-TT$_4$** (Scheme 2), which is constructed from two different symmetrically 2,5-disubstituted thiophene building blocks.[21] By replacing the thiophene heterocycle of either the divinylarylene or the dicarboxylate linker (or both) by furan or pyrrole (see Scheme 2), we successfully synthesized five new macrocyclic complexes. In particular, we used the 2,5-divinylfuran-bridged diruthenium complex **1-F** in addition to its 2,5-thiophene-bridged analogue **1-T** in self-assembly processes with thiophene-2,5-dicarboxylic acid, furan-2,5-dicarboxylic acid, and in the case of **1-T**, also pyrrole-2,5-dicarboxylic acid (Scheme 3). Despite their structural similarities, these building blocks differ slightly with respect to their intrinsic Ru-heteroatom-Ru angle. This resulted in structurally diverse macrocyclic architectures, especially when comparing the metallacycles built from **1-T** with the ones derived from

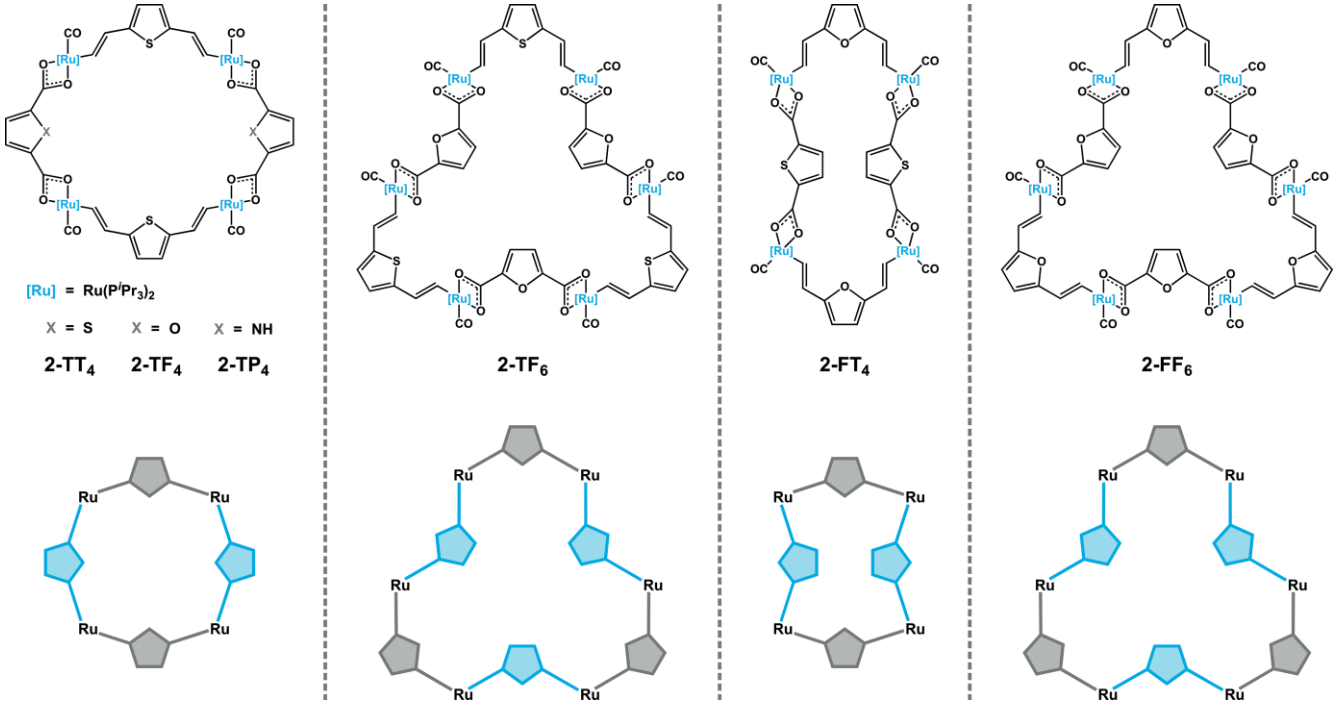

Scheme 2. The self-assembled macrocyclic structures of this study along with their graphical representations.

Full Paper
doi.org/10.1002/ejic.202000387

complex **1-F**.[22] Moreover, we present the full details of a particularly intriguing case of supramolecular isomerism[23] in metallacyclic chemistry. Thus, the reaction of **1-T** with furan-2,5-dicarboxylic acid initially leads to the exclusive formation of hexanuclear macrocycle **2-TF$_6$**, which then converts slowly and cleanly into tetranuclear **2-TF$_4$**.[24] This allowed us to compare their spectroscopic and electrochemical properties.

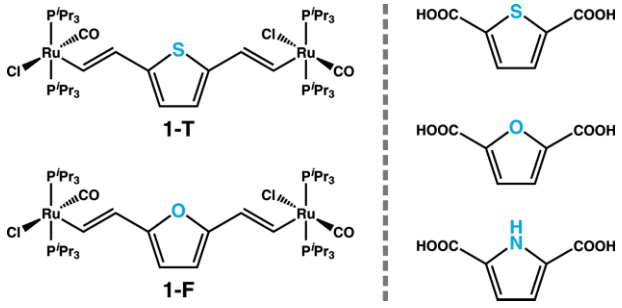

Scheme 3. The building blocks utilized in this study.

Table 1. Selected $^{31}P\{^1H\}$, ^1H and ^{13}C NMR spectroscopic data of the macrocyclic compounds and their precursor complexes **1-T** and **1-F**, measured in C_6D_6.[a]

	P^iPr_3	$H_{(1)}$ ($C_{(1)}$)	$H_{(2)}$ ($C_{(2)}$)	$H_{(4)}$ ($C_{(4)}$)	$H_{(5)}$ ($C_{(5)}$)	C_{CO} ($^2J_{C,P}$)[a]
1-T	38.49	8.60 (149.1)	6.46 (129.9)	6.40 (118.0)	–	203.9 (12.9)
2-TT$_4$	38.13	8.79 (157.3)	6.80 (130.7)	6.46 (117.4)	7.60 (131.3)	209.6 (13.6)
2-TF$_6$	37.47	8.78 (158.4)	6.70 (129.8)	6.45 (116.8)	7.15 (116.3)	209.1 (13.5)
2-TF$_4$	38.00	8.79 (157.0)	6.87 (131.2)	6.49 (117.9)	6.97 (117.0)	209.9 (13.1)
2-TP$_4$	38.07	8.69 (156.4)	6.89 (131.3)	6.50 (118.2)	6.95 (114.9)	209.8 (14.0)
1-F	38.37	8.71 (149.5)	6.27 (125.3)	5.78 (101.4)	–	204.0 (13.3)
2-FT$_4$	37.73	8.93 (156.7)	6.42 (124.9)	5.77 (100.3)	8.00 (131.1)	209.0 (13.8)
2-FF$_6$	37.22	8.74 (155.3)	6.61 (125.1)	5.99 (101.3)	6.61 (115.9)	209.3

[a] Chemical shifts are given in ppm and coupling constants in Hz.

Results and Discussion

All new macrocyclic complexes were obtained following a general synthesis route, which has so far allowed for the construction of cyclic structures from divinylphenylene-bridged diruthenium building blocks. The appropriate dicarboxylic acid is dissolved in a methanolic solution of potassium carbonate base and subsequently added to a solution containing equimolar amounts of the selected divinylarylene-bridged diruthenium precursor complex in dichloromethane. The resulting reaction mixtures were stirred for 12 h and insoluble components were removed via centrifugation. After appropriate workup, five new macrocyclic compounds were obtained as yellow (**2-TF$_6$**, **2-TP$_4$**, **2-FF$_6$**) or light red (**2-TT$_4$**, **2-FT$_4$**) solids (Scheme 2) in isolated yields of 58 % to 72 %. Detailed descriptions of the individual synthetic procedures are provided in the Supporting Information.

A summary of the new macrocyclic structures of this study and their graphical representations can be found in Scheme 2. While the family of macrocyclic compounds originating from precursor **1-T** are air- and moisture-stable in the solid state, compounds **2-FT$_4$** and **2-FF$_6$** slowly decompose upon exposure to air. All six compounds are stable in solution under inert gas atmosphere for over 24 h. Hexanuclear macrocycle **2-TF$_6$** is the noteworthy exception and undergoes slow isomerization to its tetranuclear supramolecular isomer **2-TF$_4$**.[24] The purities of all new metallamacrocycles were confirmed by NMR spectroscopy. The complete absence of resonance signals assignable to end groups of possible linear coordination polymers clearly indicates that all compounds have cyclic structures. Selected NMR data are summarized in Table 1 and the generic numbering employed for all macrocycles is detailed in Figure 1. The ^1H, $^{31}P\{^1H\}$ and ^{13}C NMR spectra are depicted in Figures S1 to S18 of the Supporting Information.

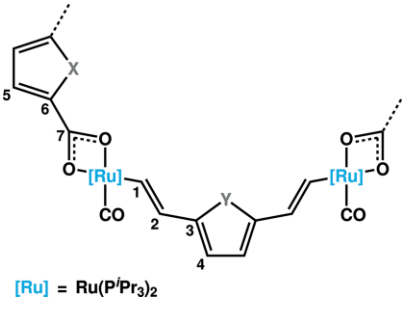

Figure 1. Systematic atom numbering for all macrocyclic complexes.

Owing to their inherently high symmetry, all metallacycles exhibit only one sharp singlet resonance in the $^{31}P\{^1H\}$ NMR spectrum, which is located between δ = 37.22 ppm and 38.13 ppm. Comparison with the parent complexes **1-T** and **1-F** reveals a slight high-field shift of the ^{31}P resonance as a consequence of the substitution of the chloride by a bidentate carboxylate ligand and the concomitant increase of the valence electron count at the metal ion from 16 to 18. This is fully consistent with previous studies on similar styrylruthenium and divinylphenylene-bridged diruthenium complexes.[17–21,25] The α and β vinyl protons $H_{(1)}$ and $H_{(2)}$ give rise to characteristic sets of doublet resonances with shift values of δ = 8.69 ppm to 8.93 ppm ($H_{(1)}$), or of 6.42 ppm to 6.89 ppm ($H_{(2)}$). The observed coupling constants range from 15.1 Hz to 15.6 Hz, which is in line with the expected *trans* geometry of the respective double bonds. Since the protons at the heterocyclic bridging ligands are chemically equivalent, they give rise to singlet resonances, whose shift values depend on the respective heterocycle. In case of compound **2-TP$_4$** the corresponding resonance signal is split into a doublet due to $^4J_{H,H}$ coupling to the pyrrolic imine proton. The latter exhibits an additional triplet resonance at δ = 9.70 ppm with the same $^4J_{H,H}$ coupling constant of 2.5 Hz. In the ^{13}C NMR spectra the characteristic triplet resonance for the carbonyl carbon atoms at δ = 209.0 ppm to 209.9 ppm is ob-

Full Paper
doi.org/10.1002/ejic.202000387

served, which is shifted by approximately 5 ppm to lower field with respect to the dinuclear precursor complexes **1-T** and **1-F**. The corresponding $^{2}J_{C,P}$ coupling constants are similar for all macrocyclic compounds and range from 13.1 Hz to 14.0 Hz.

While attesting to the high purity of the macrocycles, the NMR data provide no definitive information concerning their nuclearities. The latter were established by ultrahigh resolution mass spectrometry UHR ESI-MS, which provided the molecule ion peaks of the mono- and dications with excellent matches between the experimental and calculated isotope patterns (see Figures S19 to S24 of the Supporting Information). These studies revealed that **2-FT$_4$**, **2-TT$_4$** and **2-TP$_4$** constitute tetranuclear compounds, while **2-FF$_6$** and **2-TF$_6$** are hexanuclear in nature.

Further investigations on **2-TF$_6$** revealed a peculiar behavior. Samples recovered after unsuccessful crystallization attempts or after prolonged storage of a solution of **2-TF$_6$** in an NMR tube displayed a second set of resonances, which is also assigned to a cyclic structure (see Figure 2). Mass spectra of this mixture provided the corresponding molecule ion peaks of the original hexanuclear species **2-TF$_6$** at m/z = 3562.0790 and of its tetranuclear isomer **2-TF$_4$** at m/z = 2375.7190 with the expected isotope patterns (Figure 3). This isomerization process was subsequently followed in C_6D_6 at r. t., and a gradual conversion of **2-TF$_6$** to **2-TF$_4$** was observed over the course of several weeks. Notably, only very minor decomposition was encountered as revealed by the deposition of an only small amount of insoluble material. Pure **2-TF$_4$** could be obtained by evaporating the solvent from the filtered solution after the isomerization had gone to completion (see Figures S3, S9, S15 and S21 of the Supporting Information for its NMR and mass spectra). The time required for the isomerization was reduced to only seven days by increasing the reaction temperature to 35 °C. The limited stability of macrocycle **2-TF$_6$** in polar solvents like CH_2Cl_2 or, in particular, MeOH precludes their use in this isomerization.

The conversion of **2-TF$_6$** to **2-TF$_4$** must necessarily involve the breaking of Ru carboxylate linkages and an opening of the macrocyclic architecture. Dynamic formation and cleavage of metal-linker bonds are crucial to the formation of self-assembled macrocyclic systems and have therefore been thoroughly examined by various methods. Scrambling between bound and free ditopic diimine linkers in tetraplatinum metallacycles with anthracene- or phenanthrenediyl diplatinum linkers has been observed by isotope labeling and the mixing of labeled and unlabeled complexes, leading to heteroisotopic exchange products.[26] The addition of competing organic ligands has also been used to trigger ligand exchange processes in metallamacrocycles.[27] Moreover, Therrien and co-workers have successfully applied a combination of both these approaches.[28]

Inspired by this work, we mused that the addition of free furan-2,5-dicarboxylate (circa 1 equiv.) to macrocycle **2-TF$_6$** might accelerate its transformation to **2-TF$_4$**. By employing this approach, we were indeed able to decrease the time required for the quantitative conversion of **2-TF$_6$** to **2-TF$_4$** to 24 h. Moreover, treatment of macrocycle **2-TF$_6$** with 3 equiv. of thiophene-

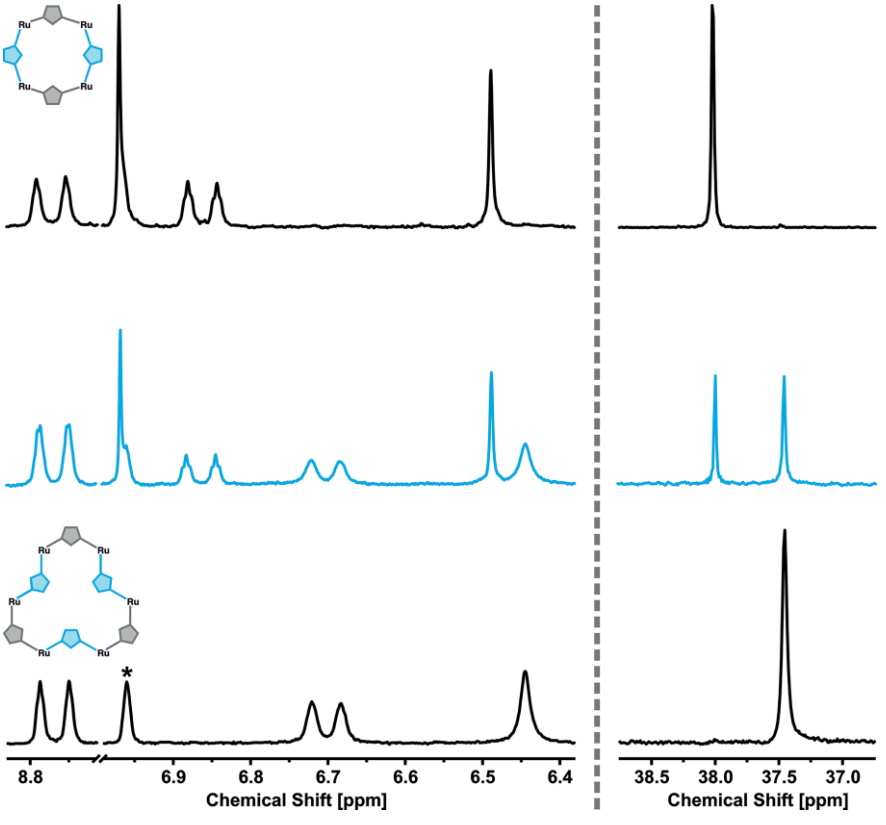

Figure 2. Excerpts from the ^{1}H NMR spectra (left) and ^{31}P{^{1}H} NMR spectra (right) of **2-TF$_4$** (top), **2-TF$_6$** (bottom) and a mixture of both supramolecular isomers that was obtained after 30 d at r. t. (middle). All spectra were recorded in C_6D_6. The peak marked with an asterisk in the bottom spectrum denotes the ^{13}C satellite peak of the solvent.

Full Paper
doi.org/10.1002/ejic.202000387

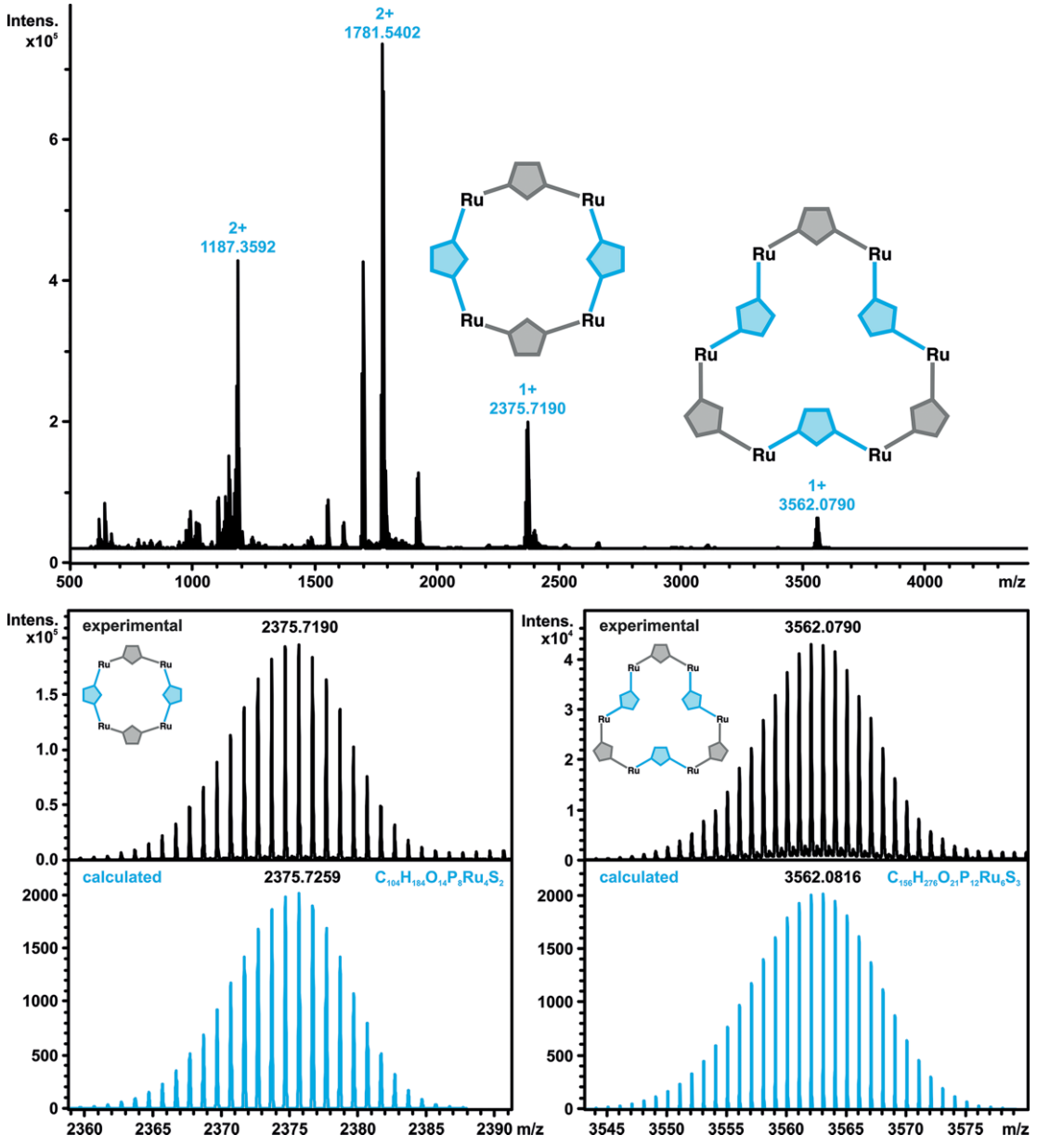

Figure 3. UHR ESI MS of a mixture of **2-TF$_6$** and **2-TF$_4$**.

2,5-dicarboxylate (one equiv. per divinylthiophene-bridged diruthenium unit) led to the exclusive formation of **2-TT$_4$** as the only detectable metal-containing product. Intrigued by this remarkable selectivity we performed a self-sorting experiment using a mixture of equimolar amounts of **1-T**, **1-F**, thiophene-2,5-dicarboxylate and furan-2,5-dicarboxylate, following the usual protocol (see the Experimental Section of the Supporting Information). In this experiment we observed the selective formation of **2-TT$_4$**, while precursor **1-F** generated a mixture of different products and partly decomposed. Since such transformations are generally thermodynamically controlled, we can safely assume that the tetranuclear compound **2-TT$_4$** represents the thermodynamically most stable product under the applied experimental conditions.

The availability of pure **2-TF$_6$** and **2-TF$_4$** allowed for a direct comparison of their NMR data. The relevant parts of the ^{1}H and the ^{31}P NMR spectra in Figure 2 reveal characteristic differences. The chemical shifts of the ^{31}P{^{1}H} NMR singlet and of the H$_{(2)}$ resonances of **2-TF$_4$** of δ = 38.00 ppm and 6.87 ppm are very similar to those of the other tetranuclear macrocycles **2-TT$_4$** and **2-TP$_4$**. In hexanuclear **2-TF$_6$**, these signals are shifted to slightly higher field of δ = 37.47 ppm and 6.70 ppm, respectively. Similar differences are also observed when comparing tetranuclear **2-FT$_4$** and hexanuclear **2-FF$_6$**, which are both derived from the divinylfuran-bridged precursor **1-F**. The ^{13}C NMR resonances also display notable differences between the supramolecular isomers **2-TF$_4$** and **2-TF$_6$**, in particular for the vinylic carbon atom C$_{(2)}$ in β-position to the Ru atoms and carbon atom C$_{(5)}$ of the thiophene-2,5-dicarboxylic acid (see Figure 1 and Table 1). The differently sized macrocycles **2-TF$_4$** and **2-TF$_6$** are also distinguished by their diffusion coefficients D of 8.85 10^{-6} cm^{2}s^{-1} or 7.73 10^{-6} cm^{2}s^{-1}, respectively, as revealed

Full Paper
doi.org/10.1002/ejic.202000387

by diffusion-ordered NMR spectroscopy (DOSY, see Figure S25 of the Supporting Information).

Final proof of the structural identities of the new metallacycles comes from X-ray crystallography. Suitable single crystals of all four tetranuclear macrocycles **2-TT$_4$**, **2-TF$_4$**, **2-TP$_4$** and **2-FT$_4$** and of hexanuclear **2-TF$_6$** were obtained by slow diffusion of methanol into a benzene solution of the respective compound. Figure 4, Figure 5 and Figure 7 depict their molecular structures. Details concerning the data collection and structure refinement as well as full lists of bond parameters can be retrieved from Tables S1 to S15 of the Supporting Information, while Figures S26 to S30 provide additional views of their structures and the atomic numbering. A selection of the most pertinent bond lengths, bond angles, torsion angles and interplanar angles is provided in Table 2. As the three tetranuclear macrocyclic structures originating from parent complex **1-T** differ only in the dicarboxylate linker, their molecular structures resemble each other closely (see Figure 4 and Table 2). They crystallize in the triclinic space group $P\bar{1}$ as benzene solvates with up to four solvent molecules per macrocyclic complex. Owing to the acute O-Ru-O angle of the four-membered carboxylate chelate ring of 58.52° to 58.85° and the concomitant opening of the C-Ru-O *cis* angles to values of 100.85(16)° to 104.2(2)° for C_{vinyl}-Ru-O, or from 106.6(2)° to 111.55(16)° for C_{CO}-Ru-O, the ruthenium atoms adopt a distorted octahedral geometry. Bond angles of *trans*-disposed ligands range from 175.47(4)° to 176.57(5)° for P-Ru-P, 165.18(16)° to 169.75(16)° for C_{CO}-Ru-O, and from 157.27(14)° to 163.34(15)° for C_{vinyl}-Ru-O. As a consequence of the larger σ-trans influence of the alkenyl ligand, the Ru-O bonds of 2.265(4) Å and 2.289(3) Å *trans* to the latter are significantly longer than those of 2.202(3) Å and 2.216(3) Å to the oxygen donors *trans* to the carbonyl ligand, similar to what has

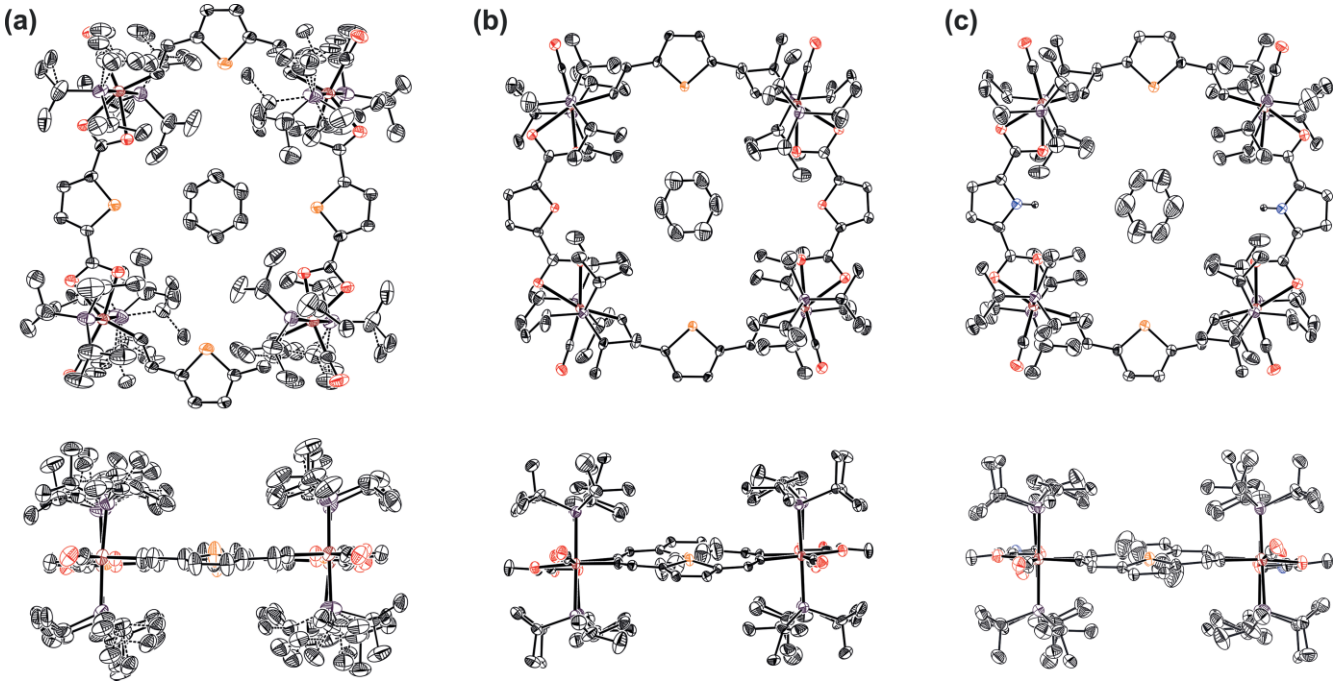

Figure 4. Top and side views of the molecular structures of the benzene solvates of **2-TT$_4$** (a), **2-TF$_4$** (b), and **2-TP$_4$** (c). Solvent molecules other than the benzene molecules in the central cavities as well as hydrogen atoms with the exception of the pyrrolic protons were removed for reasons of clarity. Thermal ellipsoids are displayed at a 50 % probability level.

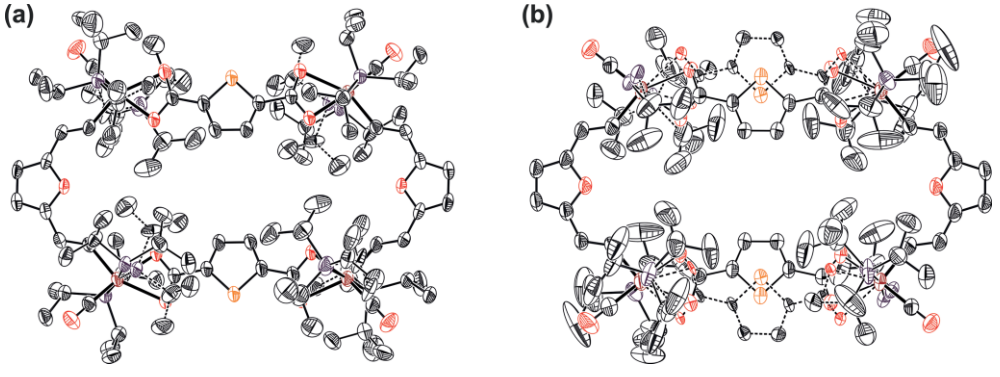

Figure 5. Molecular structures of the two independent molecules in the unit cell of macrocycle **2-FT$_4$**. The structure of the minor conformer is indicated by dotted lines. Solvent molecules and hydrogen atoms were removed for reasons of clarity. The ellipsoids are displayed at a 50 % probability level.

Table 2. Characteristic structure parameters of the macrocyclic compounds **2-TT$_4$**, **2-TF$_4$**, **2-TP$_4$** and **2-FT$_4$**[a] as benzene solvates.

	2-TT$_4$·3 C_6H_6	**2-TF$_4$**·4 C_6H_6	**2-TP$_4$**·4 C_6H_6	**2-FT$_4$**[a]·2 C_6H_6
Ru(1) - P(1)	2.4203(15)	2.4102(16)	2.3940(16)	2.4065(17)
Ru(1) - P(2)	2.4094(15)	2.4196(17)	2.4173(17)	2.4066(15)
Ru(1) - O(*trans*, CO)	2.216(3)	2.202(3)	2.214(4)	2.205(3)
Ru(1) - O(*trans*, vinyl)	2.269(3)	2.289(3)	2.265(4)	2.342(3)
Ru(1) - C(1)	2.004(5)	2.013(4)	2.016(5)	2.006(4)
Ru(1) - C(CO)	1.788(4)	1.805(5)	1.789(7)	1.799(4)
C(1) - C(2)	1.350(6)	1.349(6)	1.338(8)	1.339(5)
C(2) - C(3)	1.459(6)	1.451(6)	1.450(7)	1.436(6)
P(1) - Ru(1) - P(2)	175.47(4)	176.57(5)	176.30(6)	178.65(4)
O(1) - Ru(1) - O(2)	58.85(10)	58.52(11)	58.85(14)	58.00(10)
C(1) - C(2) - C(3)	126.6(4)	126.9(5)	128.4(5)	125.8(4)
Ru(1) - C(1) - C(2)	135.3(4)	132.0(4)	131.2(4)	138.4(3)
∡ (C_6H_6); (Ru_4)[b]	2.4	18.9	31.4	–
∡ (C_4H_2Y);[c] (Ru_4)[b]	12.1	17.6	16.9	6.2
∡ (C_4H_2X);[d] (Ru_4)[b]	2.94	6.15	7.25	23.3
torsion $\phi_{P,Ru,Ru,P}$ (vinyl)	2.5, 3.1	14.2, 14.7	14.9, 14.0	31.3, 38.0
torsion $\phi_{P,Ru,Ru,P}$ (carboxylate)	1.5, 7.2	2.6, 4.3	2.0, 3.0	1.5, 4.0
$d_{Ru,Ru}$ (vinyl)	9.9	10.4	10.4	8.3
$d_{Ru,Ru}$ (carboxylate)	10.30	9.40	9.5	10.3
Ru(1) - Ru(2) - Ru(1a)	87.2	88.0	88.2	89.4

[a] Data given for molecule 1. [b] Plane defined by the four ruthenium atoms. [c] Heterocyclic plane of the divinylarylene bridge. [d] Heterocyclic plane of the dicarboxylate linker.

been observed for other alkenylruthenium carboxylate complexes.[19–21] The vinyl groups at the divinylthiophene linkers adopt a *cisoid* conformation, and all four heteroatoms of the heterocyclic building blocks point toward the central cavity of the respective macrocycle.

The divinylthiophene linker fixes the bridged Ru atoms at a distance of 9.93 Å to 10.45 Å while the Ru···Ru distances imposed by the dicarboxylate linkers vary from 9.40 Å for the pyrrole and furan derivatives to 10.30 Å for thiophene-2,5-dicarboxylate. As a consequence of the different atomic radii of the heteroatoms and the presence of an additional proton at the pyrroles, the shapes and sizes of the inner voids of the macrocycles vary from oval with dimensions of 12.9 Å × 9.5 Å for **2-TT$_4$** to almost spherical for compounds **2-TF$_4$** and **2-TP$_4$**. The latter have inner voids with dimensions of 11.1 Å × 12.4 Å or 11.2 Å × 10.9 Å as measured between the respective heteroatoms or the pyrrolic NH protons. In all three cases, the inner void hosts a benzene solvate molecule.

For **2-TT$_4$**, the encapsulated benzene molecule is nearly coplanar to the plane defined by the four ruthenium atoms with a tilt angle of only 2.4°. Moreover, it is aligned in such a way that two opposite C-C bonds run parallel to the $C_{(5)}$-$C_{(5')}$ bond of the heterocyclic dicarboxylate linkers and two opposite C-H bonds are nearly parallel to the longer S···S vector of 12.9 Å between the sulfur atoms of the divinylthiophene linkers. In the case of macrocycles **2-TF$_4$** and **2-TP$_4$** the tilt angle between the enclosed benzene solvate molecule and the four ruthenium atoms of the macrocycle is increased to 18.9° or even to 31.4°. Furthermore, the shorter distances between the thiophene S atoms of ca. 11 Å render an alignment of the benzene solvate as in **2-TT$_4$** impossible. The benzene guest molecule thus rotates by 30° so that its HC···CH vector aligns strictly parallel to the O···O or the NH···HN axis of the dicarboxylate linkers. As the dimensions of the inner voids are still somewhat small, the heterocycles respond to benzene encapsulation with a tilt out of the plane spanned by the four Ru atoms (Table 2) and a twisting of the P-Ru-P axes in particular along the divinylthiophene-bridged sides. Such twisting is indicated by torsional angles P-Ru···Ru-P, which range from 14.0° to 14.9°. The corresponding angles in **2-TT$_4$** are much smaller with values of 2.5° and 3.1°.

As shown in Figure 5, macrocycle **2-FT$_4$** crystallizes with two independent molecules in the unit cell. One of them is well-ordered, whereas the other one exists as two different conformers with mutual occupancies of 0.84 and 0.16. For all individual structures the four ruthenium atoms define a rectangle with dimensions of 10.4 Å × 8.3 Å or 10.3 Å × 8.3 Å. The structures of molecule 1 and the major conformer of molecule 2 show remarkable differences when compared to that of its constitutional isomer **2-TF$_4$** (Figure 4, middle). At odds with the other structures the sulfur atoms of the thiophene heterocycles point outward from the inner cavity. This generates rather elongated conformations with a transannular distance of 15.1 Å or 15.2 Å between furanyl oxygen atoms and one of only 5.3 Å or 4.4 Å between opposite CH protons of the thiophenes. Such structures have already been observed in purely organic macrocycles[29] and can be explained by the acute angle Ru···O_{Furan}···Ru of 119.5° in **2-FT$_4$**, which is much smaller than that of 161.5° in its constitutional isomer **2-TF$_4$**. Comparison with values of 119.1° and 152.4° for **1-F** and **1-T**[22] shows, that the intrinsic angle Ru···O_{Furan}···Ru of their corresponding precursors are largely retained in the macrocyclic structures. The P-Ru-P vectors along the furandicarboxylate linkers are aligned in an almost parallel fashion as indicated by the torsion angles P-Ru···Ru-P of 2.6° and 4.0°, respectively. However, they are significantly tilted along the divinylthiophene units with torsion angles of 21.4° and 38.0°. As a consequence of the short transannular distance between the thiophene rings, the divinylthiophene linkers are rotated by 19.6° or 23.3° out of the Ru_4 plane. Nevertheless, the two thiophene planes remain parallel to each

Full Paper
doi.org/10.1002/ejic.202000387

other, exhibiting an interplanar distance of 3.8 Å or 4.9 Å for the two independent molecules of the unit cell. The second, minor conformer of molecule 2, represented by dotted lines in Figure 5(b), structurally resembles the other three tetranuclear macrocycles derived from precursor complex **1-T** (vide supra) and features inward-oriented thiophene linkers. Thus, this conformer has a larger inner cavity of 15.2 Å × 7.9 Å.

The coexistence of different conformers within the same unit cell suggests that their associated energy differences are rather small. In order to gain additional insight on this issue we performed quantum chemical calculations on slightly truncated model complexes with PMe_3 instead of the P^iPr_3 ligands, subsequently denoted as **2-FT$_4^{Me}$**. Both conformers are true minima on the potential hypersurface. In contrast to the experimental structures, the geometry-optimized ones display a much higher degree of coplanarity, which is probably a result of the decreased steric demands of the PMe_3 ligands. Despite these differences, the calculations reproduce the experimental trend in placing the conformer with outward-oriented thiophene rings 6.9 kJ/mol below the one with the sulfur heteroatoms oriented towards the inner void (see Figure 6). Similar calculations on macrocycle **2-TT$_4$** indicated that the conformer with inward-oriented thiophene rings is favored by a substantially larger margin of 38.9 kJ/mol, which is in excellent agreement with our experimental findings (see Figure S31 of the Supporting Information).

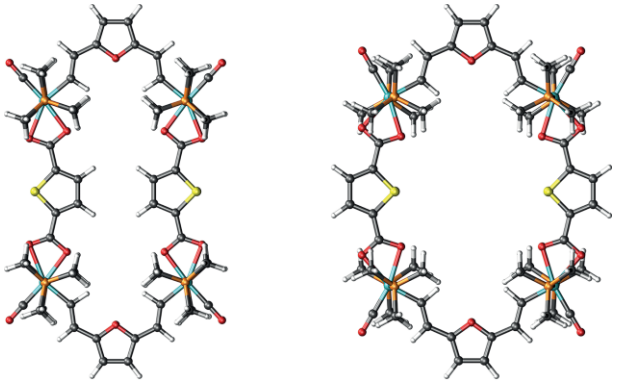

Figure 6. Calculated molecular structures of the PMe_3 models of the experimentally observed conformers of macrocycle **2-FT$_4$** and their respective energies.

The hexanuclear metallacycle **2-TF$_6$** also crystallizes in the triclinic space group $P\bar{1}$ as a benzene solvate with twelve individual solvent molecules per macrocycle. This original type of macrocyclic structure is best described as a three-pointed star-like hexagonal architecture (Figure 7). As in the major conformers of **2-FT$_4$**, the heteroatoms of the individual linkers point alternately out- or inward the central cavity. This time, however, the Ru···$S_{Thiophene}$···Ru angles between 143.8° and 147.3° at the divinylthiophene linkers are more acute than the Ru···O_{Furan}···Ru angles (range from 156.8° to 162.2°) at the furan-2,5-dicarboxylic acid linkers, such that the S atoms point inside and the O atoms outward from the inner cavity. The six crystallographically non-equivalent ruthenium atoms of **2-TF$_6$** define a slightly distorted regular hexagon with Ru···Ru separations in the range of 9.4 Å to 9.7 Å and internal Ru···Ru···Ru angles of 114.0° to 125.1°. However, in contrast to the four previously discussed molecular structures, only four ruthenium atoms of **2-TF$_6$** reside in a common plane whereas the other two are displaced by 0.6 Å or 1.2 Å above or below this plane, so that the six ruthenium atoms adopt a flat chair-like arrangement.

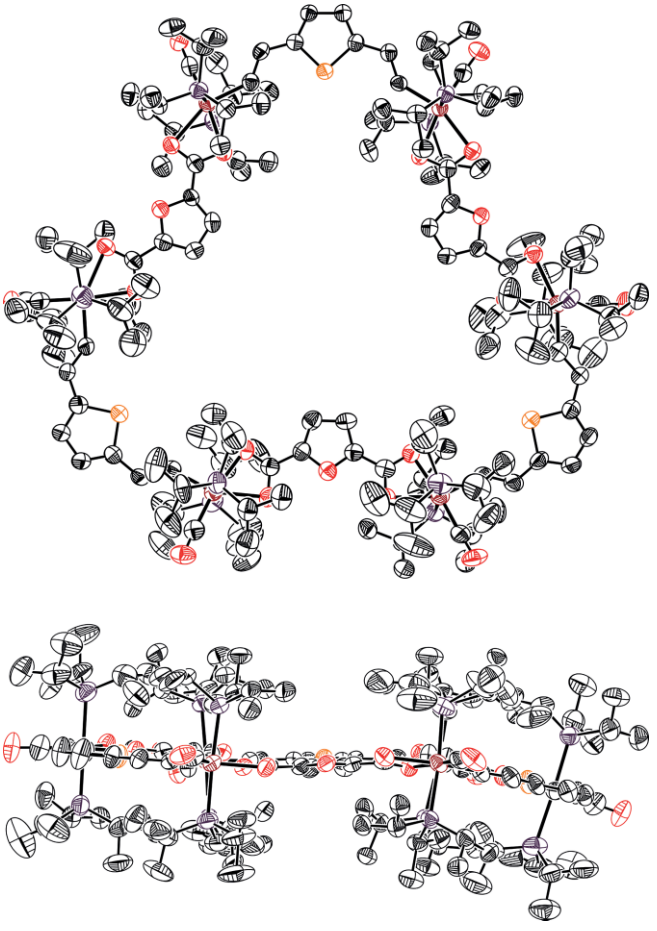

Figure 7. Top and side views of the molecular structure of the benzene solvate of macrocycle **2-TF$_6$**. Solvent molecules and hydrogen atoms were removed for reasons of clarity. The ellipsoids are displayed at a 50 % probability level.

The thiophene sulfur atoms define an almost equilateral triangle with S···S distances of 16.6 Å to 17.1 Å. Despite the different nuclearity and shape of metallacycle **2-TF$_6$**, the structural parameters of the individual vinyl ruthenium fragments match well with those found in the present and other macrocycles featuring divinylphenylene-bridged building blocks.[18–21] All six ruthenium centers adopt the same distorted octahedral geometry with O-Ru-O chelate angles of 58.13(18)° to 58.83(11)° as well as P-Ru-P angles of 173.99(9)° to 177.54(8)°. The vinyl groups of the respective divinylthiophene moieties adopt cisoid conformations. The most important difference between the two supramolecular isomers **2-TF$_6$** and **2-TF$_4$** is that the respective Ru···$S_{Thiophene}$···Ru angles between 143.8° and 147.3° at the divinylthiophene linkers in **2-TF$_6$** are appreciably smaller than that

Full Paper
doi.org/10.1002/ejic.202000387

of 161.5° in **2-TF$_4$**. These values have to be compared to that of 152.4° for precursor **1-T**. Therefore, it seems that the structural preferences of the dinuclear precursor **1-T** are better preserved in **2-TF$_6$** whereas more adjustment is necessary to obtain the structure of **2-TF$_4$**. This also coincides well with the results of self-sorting experiments (vide supra), establishing metallacycle **2-TT$_4$** as the most stable overall structure to emerge out of a mixture of various building blocks, as its corresponding Ru···S$_{Thiophene}$···Ru angle of 150.8° is almost identical to the value of precursor **1-T**. The subtle differences between the various structures highlight the conformational flexibility inherent to the individual diruthenium linkers and the macrocyclic architectures derived from them.

Moreover, we also optimized the molecular structures of the two supramolecular isomers **2-TF$_6^{Me}$** and **2-TF$_4^{Me}$** in order to compare their respective energies (see Figure S32 of the Supporting Information). In agreement with the experimental observations, the tetranuclear structure is preferred by 8.9 kJ/mol per divinylthiophene diruthenium unit. Thus, **2-TF$_6$** represents an isolable kinetic intermediate *en route* to the thermodynamically more stable tetraruthenium complex **2-TF$_4$**.[24]

As we did so far not succeed in obtaining suitable single crystals of the exclusively furan based hexanuclear macrocycle **2-FF$_6$**, we resorted to quantum chemical modeling of its simplified PMe$_3$ model **2-FF$_6^{Me}$** (see Figure S33 of the Supporting Information). At first glance the geometry-optimized structure of **2-FF$_6^{Me}$** is quite similar to the experimentally determined structure of hexanuclear macrocycle **2-TF$_6$** (vide supra). The six ruthenium centers also define an almost regular hexagon with Ru···Ru distances ranging from 8.8 Å to 9.6 Å and internal Ru···Ru···Ru angles of 119.3° to 120.9°.

However, there is a significant difference between the two hexanuclear structures, as the Ru···O$_{Furan}$···Ru angles defined by the ruthenium ions and the oxygen atom of the divinylfuran linkers of 127.2° to 127.6° in the calculated structure of **2-FF$_6^{Me}$** are significantly more acute than the respective Ru···S$_{Thiophene}$···Ru angles of 143.5° to 147.3° in metallacycle **2-TF$_6$**.

The electrochemical properties of the new ruthenium metallamacrocycles resemble each other closely, irrespective of their different nuclearities. In every case, the voltammograms feature two consecutive, reversible oxidations. Every apparent wave consists of two or three closely-spaced one-electron processes (see left panel of Figure 8) due to the stepwise charging of the mutually insulated divinylarylene-bridged diruthenium entities. For **2-TT$_4$**, **2-TF$_4$** and **2-TP$_4$** some small splitting of the first composite wave into two individual one-electron processes can be discerned in the CH_2Cl_2/NBu_4PF_6 supporting electrolyte. Replacing PF_6^- by the even less ion pairing $[B\{C_6H_3(CF_3)_2\text{-}3,5\}_4]^-$ (BAr^{F24}) anion generally enhances the redox splittings $\Delta E_{1/2}$. In some cases, small splittings of also the second oxidation waves are noted in this electrolyte (see Figures S34 to S51 and Tables S16 to S21 of the Supporting Information). This however, comes with a distinct broadening of particularly the second composite oxidation waves, obviously as the result of more sluggish electron transfer kinetics. A similar non-ideal behavior imposed by the BAr^{F24} anion has been noted very recently.[30]

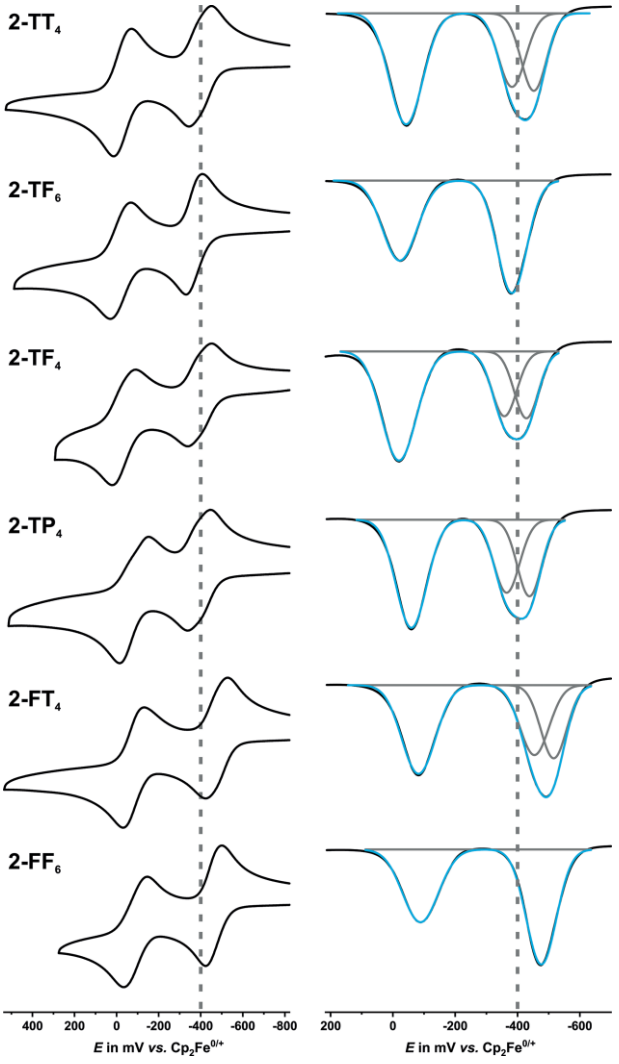

Figure 8. Cyclic (left, v = 100 mVs^{-1}) and square wave voltammograms (right) of all six macrocyclic compounds, measured in CH_2Cl_2/0.1 M $^nBu_4NPF_6$, along with deconvolutions. Dotted grey lines were included as a guide to the eye.

Half-wave potentials $E_{1/2}$ as derived from the cyclic voltammograms or from deconvolution of the respective square wave voltammograms are listed for both supporting electrolytes in Table 3. Comparison with their respective precursor complexes **1-T** and **1-F** reveals cathodic shifts of the first composite waves by ca. 150 mV and smaller ones of ca. 60 mV for the second charging of the divinylarylene diruthenium entities to their corresponding dications in the metallamacrocycles. This is the expected consequence of increasing the valence electron count at the ruthenium centers from 16 to 18 concomitant with the substitution of chloride by carboxylate ligands.[17–21] As for their dinuclear precursors, the more electron rich, furan-based macrocycles **2-FT$_4$** and **2-FF$_6$** oxidize at ca. 60 mV lower potentials than their divinylthiophene counterparts derived from **1-T**. The influence of the respective dicarboxylate linker is, however, only small.

Direct comparison of the two supramolecular isomers **2-TF$_4$** and **2-TF$_6$** reveals that the oxidation potential of the first composite wave of the former is by ca. 20 mV lower while there is no notable effect on the second wave. Moreover, no apparent

Full Paper
doi.org/10.1002/ejic.202000387

Table 3. Half-wave potentials of all macrocyclic compounds and their dinuclear precursor complexes **1-T** and **1-F** in mV vs. $Cp_2Fe^{0/+}$.[a]

	$E_{1/2}^{0/+}$	$E_{1/2}^{+/2+}$	$E_{1/2}^{2+/3+}$	$E_{1/2}^{3+/4+}$	$E_{1/2}^{4+/5+}$	$E_{1/2}^{5+/6+}$
1-T	–294 (–360)	36 (–10)	–	–	–	–
1-F	–385 (–455)	–20 (–50)	–	–	–	–
2-TT$_4$	–452 (–547)	–382 (–477)	–43 (–91)	–43 (–14)	–	–
2-TF$_6$	–382 (–476)	–382 (–476)	–382 (–476)	–22 (–75)	–22 (–13)	–22 (122)
2-TF$_4$	–429 (–529)	–358 (–458)	–20 (–91)	–20 (13)	–	–
2-TP$_4$	–438 (–521)	–365 (–453)	–59 (–60)	–59 (91)	–	–
2-FT$_4$	–516 (–600)	–454 (–552)	–82 (–72)	–82 (144)	–	–
2-FF$_6$	–477 (–559)	–477 (–559)	–477 (–559)	–89 (–134)	–89 (–54)	–89 (136)

[a] In CH_2Cl_2/^{n}Bu$_4$NPF$_6$; (in CH_2Cl_2/^{n}Bu$_4$NBAr^{F24}).

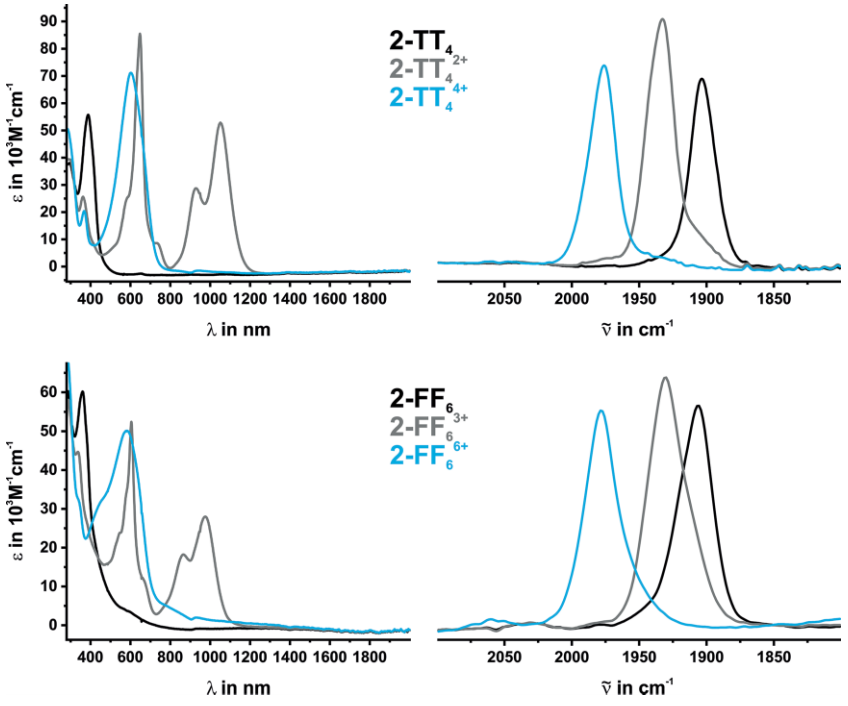

Figure 9. Changes in the UV/Vis/NIR spectra (left) and the *ν*(CO) region of the IR spectra (right) during stepwise oxidation of **2-TT$_4$** (top) and **2-FF$_6$** (bottom).

splitting of even the first composite wave into individual one-electron processes is discernible for the hexanuclear macrocycles.

In order to gain further insight into the electronic properties of the present metallamacrocyclic complexes, we also monitored the evolution of their IR and UV/Vis/NIR spectra in response to the individual redox processes. As the electrolysis takes much longer than voltammetric measurements (vide supra), these experiments also provide additional information regarding the redox stability of the investigated compounds on an extended timescale.

Figure 9 compares the results of UV/Vis/NIR and IR spectroelectrochemical investigations of tetranuclear macrocycle **2-TT$_4$** and its furan-based hexanuclear counterpart **2-FF$_6$**. Complete sets of spectra for all six macrocyclic compounds can be found as Figures S52 to S75 of the Supporting Information; corresponding data are summarized in Table 4.

The energy changes of the CO stretching vibrations ν(CO) of the ruthenium-bonded carbonyl ligands provide a convenient handle to monitor the electron density changes at the respective ruthenium ions by IR spectroscopy. All six macrocyclic compounds exhibit almost identical energies of their respective ν(CO) bands in their corresponding oxidation states. Closer inspection reveals slightly higher energies $\tilde{\nu}_{CO}$ of 1907 cm^{-1} (**2-FF$_6$**) or 1906 cm^{-1} (**2-TF$_6$**) for the two hexanuclear macrocycles as compared to those of 1903 cm^{-1} for their tetraruthenium counterparts. During the first composite oxidation this band shifts by roughly 30 cm^{-1} to higher energy. This is accompanied by the growth of intense structured bands at 800 to 1200 nm in the near infrared (NIR), as well as of an even more intense Vis band peaking at ca 650 nm. The former are due to the electronic HOMO → LUMO (or, more specifically, the β-HOSO → β-LUSO) transitions between delocalized MOs that extend over the individual open-shell diruthenium divinylarylene chromophores.[31] The electronic bands of the open-shell di- or trications, i.e. after unipositive charging of every divinylarylene-bridged subunit of the respective macrocycle, are basically superimposable to those of their corresponding one-electron oxidized monocationic precursor complexes **1-T$^+$** or **1-F$^+$**, thus indicating complete charge delocalization within every divinylarylene-bridged diruthenium fragment.[22] However, no specific spectroscopic signature for any intermediately formed

Full Paper
doi.org/10.1002/ejic.202000387

Table 4. Characteristic spectroscopic data for all macrocyclic compounds as well as their dinuclear precursor complexes **1-T** and **1-F** in all accessible oxidation states.

	$\tilde{\nu}_{CO}$ in cm^{-1}	λ in nm (ε_{max} in 10^3 L mol^{-1} cm^{-1})
1-T	1911	600 (1.3), 410 (32.0), 392 (38.5)
1-T^{+}	1937	1040 (35.8), 916 (16.0), 643 (44.8),
1-T^{2+}	1979	612 (45.5)
2-TT$_4$	1903	389 (56.1)
2-TT$_4$ $^{2+}$	1933	1051 (53.0), 929 (29.0), 648 (85.8)
2-TT$_4$ $^{4+}$	1976	603 (71.5)
2-TF$_6$	1906	391 (76.2)
2-TF$_6$ $^{3+}$	1935	1051 (64.2), 923 (34.4), 647 (107.9)
2-TF$_6$ $^{6+}$	1976	612 (113.8)
2-TF$_4$	1905	391 (50.7)
2-TF$_4$ $^{2+}$	1932	1050 (42.2), 930 (21.2), 646 (72.1)
2-TF$_4$ $^{4+}$	1975	607 (76.4)
2-TP$_4$	1903	392 (59.1)
2-TP$_4$ $^{2+}$	1933	1063 (48.4), 938 (28.5), 650 (82.4)
2-TP$_4$ $^{4+}$	1974	606 (105.4)
1-F	1909	570 (2.0), 366 (28.5)
1-F^{+}	1936	960 (19.5), 956 (12.5), 591 (28.8)
1-F^{2+}	1978	574 (26.6)
2-FT$_4$	1903	356 (53.2)
2-FT$_4$ $^{2+}$	1932	980 (40.4), 866 (28.2), 604 (71.0)
2-FT$_4$ $^{4+}$	1977	579 (67.8)
2-FF$_6$	1907	360 (58.8)
2-FF$_6$ $^{3+}$	1931	976.3 (28.1), 866 (18.3), 605 (54.4)
2-FF$_6$ $^{6+}$	1978	583 (50.1)

radical cation or, in the case of the hexanuclear complexes, radical cation and dication can be identified in the spectra, even though these species constitute the major constituents in the solution at some point of the electrolysis. This argues against any detectable through-bond or through-space interactions between the conjugated divinylarylene diruthenium moieties, which is due to the insulating character of the dicarboxylate linkers. We can therefore conclude that the small redox splittings of the composite waves into individual one-electron processes are entirely due to electrostatic interactions. On further oxidizing the di- or trications to the tetra- or hexacationic species, each with two or three dicationic divinylarylene-bridged diruthenium entities, the respective Ru(CO) IR band experiences a further blue-shift. This is accompanied by a bleach of the structured NIR band and a broadening and slight shifting of the prominent Vis absorption. Such behavior is fully consistent with our previous observations on the second oxidation of their dinuclear precursor complexes.

Our experimental findings fully agree with the results of quantum chemical calculations conducted on the model complex **2-TT$_4$^{Me}** with PMe_3 instead of P^iPr_3 ligands. Figure 10 displays contour diagrams of the corresponding frontier orbitals and their associated energy levels. The so-called "redox orbitals" HOMO and HOMO-1 are both doubly degenerate and represent the in- and out-of-phase combinations of MOs which are delocalized over every separate divinylthiophene diruthenium unit and do not exhibit any contributions of the dicarboxylate linkers. This is consistent with our previous results on similar macrocycles with divinylphenylene diruthenium building blocks.[17–19] The lack of any energy splitting between the in- and out-of-phase combinations is a clear token of the lack of electronic

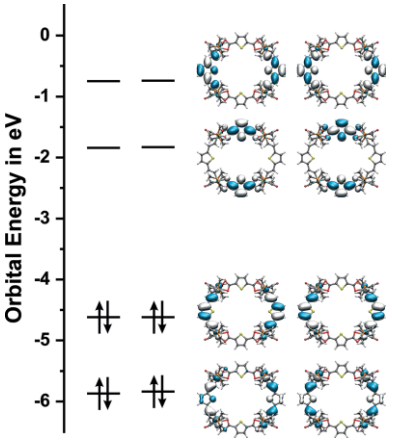

Figure 10. Partial MO scheme including graphical representations of frontier MOs of model compound **2-TT$_4$^{Me}**.

interactions between the π-conjugated divinylarylene diruthenium subunits.

EPR spectroscopy provides valuable information on the metal/ligand character of the respective SOMOs of paramagnetic systems and on the degree of spin delocalization in open-shell mixed-valent compounds. For EPR studies, the dicationic forms of all four tetranuclear macrocycles as well as the trications of the two hexanuclear complexes were prepared via chemical oxidation with either 2 or 3 equiv. of ferrocenium hexafluorophosphate, whereas the corresponding tetra- or hexacations were generated by using an excess amount (> 4 equiv. or > 6 equiv., respectively) of acetylferrocenium hexafluoroantimonate as the oxidizing agent.

Before being subjected to EPR measurements, the identities of the samples were confirmed by the match of their IR/NIR spectra with those obtained in our spectroelectrochemical experiments. Representative EPR spectra of the oxidized forms of complexes **2-TT$_4$** and **2-FF$_6$** are depicted in Figure 11; the spec-

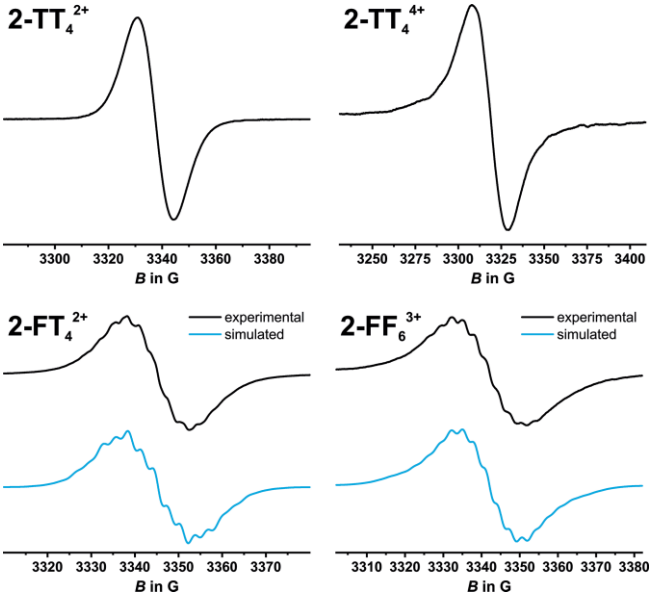

Figure 11. EPR spectra of **2-TT$_4$$^{2+}$** (top left), **2-TT$_4$$^{4+}$** (top right) as well as experimental and simulated spectra of **2-FT$_4$$^{2+}$** (bottom left) and **2-FF$_6$$^{3+}$** (bottom right), measured in CH_2Cl_2 at room temperature.

tra of all other oxidized macrocyclic complexes can be found in Figures S76 to S81 of the Supporting Information. Corresponding data are summarized in Table 5.

Table 5. EPR parameters for all oxidized macrocyclic compounds as well as their dinuclear precursor complexes **1-T**$^{+}$ and **1-F**$^{+}$.[a]

	g_{iso}	$A(^{31}P)$ (4 P)	$A(^{99/101}Ru)$ (2 Ru)	$A(^{1}H)$ (2 H)	$A(^{1}H)$ (2 H)
1-T^{+}	2.019	9.3	4.1	2.6	1.3
2-TT$_4$ $^{2+}$	2.012	–	–	–	–
2-TT$_4$ $^{4+}$	2.023	–	–	–	–
2-TF$_6$ $^{3+}$	2.012	–	–	–	–
2-TF$_6$ $^{6+}$	2.023	–	–	–	–
2-TF$_4$ $^{2+}$	2.012	–	–	–	–
2-TF$_4$ $^{2+}$	2.023	–	–	–	–
2-TP$_4$ $^{2+}$	2.012	–	–	–	–
2-TP$_4$ $^{4+}$	2.024	–	–	–	–
1-F^{+}	2.017	10.7	1.4	5.2	2.7
2-FT$_4$ $^{2+}$	2.009	7.8	5.4	5.0	3.1
2-FT$_4$ $^{4+}$	2.019	–	–	–	–
2-FF$_6$ $^{3+}$	2.010	7.9	8.7	4.3	3.8
2-FF$_6$ $^{6+}$	2.019	–	–	–	–

[a] Hyperfine coupling constants in Gauss.

In agreement with previous work, the dications of the three divinylthiophene-based tetranuclear macrocycles **2-TT$_4$**$^{2+}$, **2-TF$_4$**$^{2+}$ and **2-TP$_4$**$^{2+}$ are EPR active and exhibit an isotropic signal at a g_{iso}-value of 2.012 without any resolved hyperfine splitting.[17–21] The EPR spectrum of hexanuclear **2-TF$_6$**$^{3+}$ is basically superimposable with that of its tetranuclear isomer **2-TF$_4$**$^{2+}$.

However, the di- or trications **2-FT$_4$**$^{2+}$ and **2-FF$_6$**$^{3+}$ of the two macrocyclic complexes derived from furan-2,5-diyl-bridged **1-F** show resolved hyperfine splittings (hfs). The experimental spectra are well reproduced by assuming hfs constants $A(^{31}P)$ of 7.8 G or 7.9 G to four equivalent phosphorus atoms and $A(^{99/101}Ru)$ of 5.4 G or 8.7 G for **2-FT$_4$**$^{2+}$ and **2-FF$_6$**$^{3+}$, respectively, as well as additional hfs's to two Ru nuclei different pairs of protons (Figure 11 and Table 5). These values fall in the range of those observed for similar diruthenium complexes, where an unpaired spin is completely delocalized over a [{Ru}-CH=CH-heterocycle-CH=CH-{Ru}]$^{+}$ moiety. No delocalization between the individual divinyldiruthenium units, however, ensues. This agrees with the results of our IR and UV/Vis/NIR investigations and further underscores the electronically insulating character of the dicarboxylate linkers.

Our experimental findings also match with the computed spin densities of the mono- and dicationic forms of the model compound **2-TT$_4$**^{Me} (see Figure 12). In the case of monocation **2-TT$_4$**$^{Me+}$ the unpaired spin density is confined to just one divinylthiophene diruthenium moiety. In the corresponding dication **2-TT$_4$**$^{Me2+}$ both conjugated sides host the same spin density. In both cases, the dicarboxylate linkers are completely devoid of any unpaired spin density.

In contrast to many dioxidized 1,4-divinylphenylene-bridged diruthenium complexes, the dications of the precursor complexes **1-T**$^{2+}$ and **1-F**$^{2+}$ are EPR silent.[17,22] They thus conform to Ovchinnikov's rule, which predicts a singlet ground state with a quinoidally distorted divinylarylene linker instead of an open-shell biradical structure (see Figure 13).[32,33] The dioxidized divinylphenylene-bridged congener, however, possesses a para-

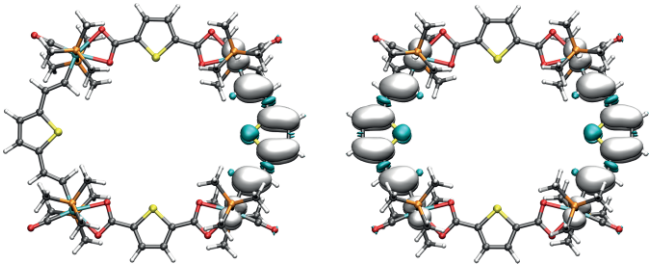

Figure 12. Calculated spin densities for **2-TT$_4$**$^{Me+}$ (left) as well as **2-TT$_4$**$^{Me2+}$ (left).

magnetic ground-state with two unpaired spins. This dichotomy obviously relates to the lower aromatic resonance energies of the furan- and thiophene heterocycles as compared to that of benzene.[34] In line with this view, dicationic divinylnaphthalene- and divinylbenzothiadiazole-bridged diruthenium complexes also adopt a diamagnetic ground state.[32]

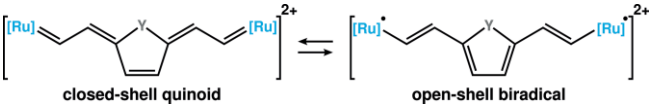

Figure 13. Possible spin states and electronic structures of a dioxidized divinylheterocycle-bridged diruthenium complex.

Quite to our surprise, the tetra- or hexacations of all six macrocyclic compounds were found to be EPR active in solution, albeit providing a much less intense signal as equally concentrated solutions of the corresponding di- or trications. Thus, we can conclude that a doubly oxidized divinylthiophene or -furan-bridged diruthenium complex, in this structural environment, exists at least partially in an EPR active, open-shell biradical state. The latter becomes obviously feasible through the enhanced propensity of the (RCOO)(P^{i}Pr$_3$)$_2$(CO)Ru-CH=CH- entities to host unpaired spin density, which then allows the heterocyclic linkers to retain their aromatic character even after twofold oxidation.

Conclusions

We have successfully self-assembled divinylthiophene- or divinylfuran-bridged diruthenium complexes and thiophene-, furan- or pyrrole-2,5-dicarboxylate linkers to symmetric, macrocyclic tetra- or hexaruthenium complexes. Five such metallamacrocycles were cleanly generated in yields of up to 72 %. Their purities were confirmed by ^{1}H, ^{13}C and ^{31}P{^{1}H} NMR spectroscopy while the UHR ESI-MS data disclose their respective nuclearities. Furthermore, we were able to obtain single crystals of five of these macrocycles and to determine their structures by X-ray crystallography. Whereas the molecular structures of the three tetranuclear compounds that originate from the thiophene-bridged complex **1-T** differ only slightly from each other, macrocycle **2-FT$_4$** prefers an elongated conformation in the solid state, where the sulfur heteroatoms

of the thiophene-2,5-dicarboxylate linkers point outward the central cavity. This particular conformation is also found in the molecular structure of hexanuclear metallacycle **2-TF$_6$**, thus generating a three-pointed star-like architecture.

Moreover, we report a remarkable case of supramolecular isomerism in metallamacrocyclic chemistry. Thus, the initially formed hexanuclear complex **2-TF$_6$** constitutes an isolable kinetic isomer, which slowly, but cleanly, transforms into the thermodynamically more stable tetranuclear isomer **2-TF$_4$**. This isomerization occurs over the course of three months in C_6D_6 at r. t., while taking seven days at 35 °C. In the presence of the free dicarboxylate ligand, this process is much faster and goes to completion within one day. The hypothesis that **2-TF$_6$** forms in a kinetically controlled process while **2-TF$_4$** constitutes the thermodynamically more favorable species finds support from the results of quantum chemical calculations.

We also studied the electrochemical and spectroscopic properties of all six macrocyclic complexes by means of cyclic and square wave voltammetry, IR and UV/Vis/NIR spectroelectrochemistry as well as EPR spectroscopy. We were able to show that their mixed-valent forms comprise of two or three intrinsically delocalized divinylarylene-bridged diruthenium entities, which are mutually interconnected by electronically insulating dicarboxylate linkers. Furthermore, all of their oxidized forms are EPR active. While this is expected for the di- or trications of the tetra- or hexanuclear complexes with unipositively charged divinylarylene-bridged diruthenium entities, the EPR activity of their tetra- and hexacations, albeit weak, indicates at the relevance of open shell structures.

The tetranuclear metallamacrocycles can be regarded as organometallic versions of thiacrown ethers with S_4, S_2O_2, or $S_2(NH)_2$ donor sets. Translation of the rich coordination chemistry of such macrocyclic ligands to the present structures is, however, no trivial task as transannular S···S distances of the latter are more than twice as large.[35] Careful adaptation of the shapes and sizes and complementary functionalization as to provide specific attractive interactions between the host metallamacrocycle and the respective guest are therefore needed to achieve reasonably strong and selective guest binding inside the central cavity. Work along these lines is presently being pursued in our laboratories.

Experimental Section

Detailed information can be found in the Supporting Information. The document includes all synthetic procedures, characterization data, NMR and mass spectra, cyclic and square wave voltammograms, results of IR and UV/Vis/NIR spectroelectrochemical measurements with deconvolutions as well as EPR spectra and quantum chemical calculations.

Deposition Number(s) 1819561 (for **2-TT$_4$**), 1961606 (for **2-TF$_6$**), 1961607 (for **2-TF$_4$**), 1961725 (for **2-TP$_4$**), and 1961726 (for **2-FT$_4$**) contain(s) the supplementary crystallographic data for this paper. These data are provided free of charge by the joint Cambridge Crystallographic Data Centre and Fachinformationszentrum Karlsruhe Access Structures service www.ccdc.cam.ac.uk/structures.

Acknowledgments

This work was supported by the bwHPC program through the computational resources of the bwUniCluster and the JUSTUS HPC facility. We also thank Sebastian Sutter and Prof. Dr. Sebastian Polarz from the Universität Konstanz for the acquisition of additional ESI-MS spectra. Open access funding enabled and organized by Projekt DEAL.

Keywords: Metallamacrocycles · Heterocycles · Supramolecular isomerism · (Spectro)electrochemistry · Electrochromism

[1] P. Stricklen, J. Verkade, *J. Am. Chem. Soc.* **1983**, *105*, 2494.
[2] a) T. R. Cook, P. J. Stang, *Chem. Rev.* **2015**, *115*, 7001; b) M. Han, D. M. Engelhard, G. H. Clever, *Chem. Soc. Rev.* **2014**, *43*, 1848; c) M. M. J. Smulders, I. A. Riddell, C. Browne, J. R. Nitschke, *Chem. Soc. Rev.* **2013**, *42*, 1728; d) R. Chakrabarty, P. S. Mukherjee, P. J. Stang, *Chem. Rev.* **2011**, *111*, 6810; e) B. Lippert, P. J. Sanz Miguel, *Chem. Soc. Rev.* **2011**, *40*, 4475; f) Y.-F. Han, W.-G. Jia, W.-B. Yu, G.-X. Jin, *Chem. Soc. Rev.* **2009**, *38*, 3419; g) P. H. Dinolfo, S.-S. Sun, J. T. Hupp in *Encyclopedia of Supramolecular Chemistry* (Eds.: J. L. Atwood, J. W. Steed), CRC Press, Boca Raton, Florida, **2004**, pp. 909–916; h) M. M. Siddiqui, R. Saha, P. S. Mukherjee, *Inorg. Chem.* **2019**, *58*, 4491; i) J. Singh, D. H. Kim, E.-H. Kim, N. Singh, H. Kim, R. Hadiputra, J. Jung, K.-W. Chi, *Chem. Commun.* **2019**, *55*, 6866; j) Y. H. Song, N. Singh, J. Jung, H. Kim, E.-H. Kim, H.-K. Cheong, Y. Kim, K.-W. Chi, *Angew. Chem.* **2016**, *128*, 2047; *Angew. Chem. Int. Ed. Engl.* **2016**, *55*, 2007; k) H. Lee, P. Elumalai, N. Singh, H. Kim, S. U. Lee, K.-W. Chi, *J. Am. Chem. Soc.* **2015**, *137*, 4674.
[3] a) S. Shanmugaraju, S. A. Joshi, P. S. Mukherjee, *Inorg. Chem.* **2011**, *50*, 11736; b) S. Shanmugaraju, A. K. Bar, K.-W. Chi, P. S. Mukherjee, *Organometallics* **2010**, *29*, 2971.
[4] a) V. Martínez-Agramunt, S. Ruiz-Botella, E. Peris, *Chem. Eur. J.* **2017**, *23*, 6675; b) D.-H. Qu, Q.-C. Wang, Q.-W. Zhang, X. Ma, H. Tian, *Chem. Rev.* **2015**, *115*, 7543; c) A. Schmidt, A. Casini, F. E. Kühn, *Coord. Chem. Rev.* **2014**, *275*, 19; d) A. Mishra, S. C. Kang, K.-W. Chi, *Eur. J. Inorg. Chem.* **2013**, *2013*, 5222; e) R. Custelcean, *Chem. Soc. Rev.* **2014**, *43*, 1813; f) S. Dhara, M. A. Ansari, G. K. Lahiri, *Inorg. Chem.* **2019**, *58*, 10991.
[5] a) G. Gupta, G. S. Oggu, N. Nagesh, K. K. Bokara, B. Therrien, *CrystEngComm* **2016**, *18*, 4952; b) E. Orhan, A. Garci, T. Riedel, P. J. Dyson, B. Therrien, *J. Org. Chem.* **2016**, *815–816*, 53; c) B. Therrien, J. Furrer, *Adv. Chem.* **2014**, *2014*, 1; d) J. E. M. Lewis, E. L. Gavey, S. A. Cameron, J. D. Crowley, *Chem. Sci.* **2012**, *3*, 778; e) A. Schmidt, V. Molano, M. Hollering, A. Pöthig, A. Casini, F. E. Kühn, *Chem. Eur. J.* **2016**, *22*, 2253; f) Y.-R. Zheng, K. Suntharalingam, T. C. Johnstone, S. J. Lippard, *Chem. Sci.* **2015**, *6*, 1189; g) H. S. Song, Y. H. Song, N. Singh, H. Kim, H. Jeon, I. Kim, S. C. Kang, K.-W. Chi, *Sci. Rep.* **2019**, *9*, 242; h) J.-H. Jo, N. Singh, D. Kim, S. M. Cho, A. Mishra, H. Kim, S. C. Kang, K.-W. Chi, *Inorg. Chem.* **2017**, *56*, 8430; i) P. Elumalai, Y. J. Jeong, D. W. Park, D. H. Kim, H. Kim, S. C. Kang, K.-W. Chi, *Dalton Trans.* **2016**, *45*, 6667; j) N. Singh, S. Jang, J.-H. Jo, D. H. Kim, D. W. Park, I. Kim, H. Kim, S. C. Kang, K.-W. Chi, *Chem. Eur. J.* **2016**, *22*, 16157; k) A. Dubey, Y. J. Jeong, J. H. Jo, S. Woo, D. H. Kim, H. Kim, S. C. Kang, P. J. Stang, K.-W. Chi, *Organometallics* **2015**, *34*, 4507.
[6] A. Garci, J.-P. Mbakidi, V. Chaleix, V. Sol, E. Orhan, B. Therrien, *Organometallics* **2015**, *34*, 4138.
[7] a) M. Yoshizawa, J. K. Klosterman, M. Fujita, *Angew. Chem. Int. Ed.* **2009**, *48*, 3418; b) S. Horiuchi, T. Murase, M. Fujita, *Chem. Asian J.* **2011**, *6*, 1839.
[8] a) R. F. Winter, *Curr. Op. Electrochem.* **2018**, *8*, 14; b) V. Croué, S. Goeb, M. Sallé, *Chem. Commun.* **2015**, *51*, 7275.
[9] a) P. H. Dinolfo, V. Coropceanu, J. Brédas, J. T. Hupp, *J. Am. Chem. Soc.* **2006**, *128*, 12592; b) P. H. Dinolfo, S. J. Lee, V. Coropceanu, J. Brédas, J. T. Hupp, *Inorg. Chem.* **2005**, *44*, 5789; c) P. H. Dinolfo, J. T. Hupp, *J. Am. Chem. Soc.* **2004**, *126*, 16814; d) P. H. Dinolfo, M. E. Williams, C. L. Stern, J. T. Hupp, *J. Am. Chem. Soc.* **2004**, *126*, 12989.
[10] a) M. Gaschard, F. Nehzat, T. Cheminel, B. Therrien, *Inorganics* **2018**, *6*, 97; b) V. Vajpayee, S. Bivaud, S. Goeb, V. Croué, M. Allain, B. V. Popp, A. Garci, B. Therrien, M. Sallé, *Organometallics* **2014**, *33*, 1651; c) M. Yuan,

F. Weisser, B. Sarkar, A. Garci, P. Braunstein, L. Routaboul, B. Therrien, *Organometallics* **2014**, *33*, 5043; d) J. Mattsson, P. Govindaswamy, A. K. Renfrew, P. J. Dyson, P. Štěpnička, G. Süss-Fink, B. Therrien, *Organometallics* **2009**, *28*, 4350; e) M. Fujita, M. Tominaga, A. Hori, B. Therrien, *Acc. Chem. Res.* **2005**, *38*, 369.
[11] S. Krykun, M. Allain, V. Carré, F. Aubriet, Z. Voitenko, S. Goeb, M. Sallé, *Inorganics* **2018**, *6*, 44.
[12] a) W. Kaim, B. Schwederski, A. Dogan, J. Fiedler, C. J. Kuehl, P. J. Stang, *Inorg. Chem.* **2002**, *41*, 4025; b) H. Hartmann, S. Berger, R. Winter, J. Fiedler, W. Kaim, *Inorg. Chem.* **2000**, *39*, 4977.
[13] V. Hoffmann, L. Le Pleux, D. Häussinger, O. T. Unke, A. Prescimone, M. Mayor, *Organometallics* **2017**, *36*, 858.
[14] a) L. E. Wilson, C. Hassenrück, R. F. Winter, A. J. P. White, T. Albrecht, N. J. Long, *Angew. Chem. Int. Ed.* **2017**, *56*, 6838; b) M. S. Inkpen, S. Scheerer, M. Linseis, A. J. P. White, R. F. Winter, T. Albrecht, N. J. Long, *Nat. Chem.* **2016**, *8*, 825.
[15] a) V. Kunz, M. Schulze, D. Schmidt, F. Würthner, *ACS Energy Lett.* **2017**, *2*, 288; b) M. Schulze, V. Kunz, P. D. Frischmann, F. Würthner, *Nat. Chem.* **2016**, *8*, 576.
[16] a) G. Szalóki, S. Krykun, V. Croué, M. Allain, Y. Morille, F. Aubriet, V. Carré, Z. Voitenko, S. Goeb, M. Sallé, *Chem. Eur. J.* **2018**, *24*, 11273; b) G. Szalóki, V. Croué, V. Carré, F. Aubriet, O. Alévêque, E. Levillain, M. Allain, J. Aragó, E. Ortí, S. Goeb et al., *Angew. Chem. Int. Ed.* **2017**, *56*, 16272; c) V. Croué, S. Goeb, G. Szalóki, M. Allain, M. Sallé, *Angew. Chem. Int. Ed.* **2016**, *55*, 1746.
[17] S. Scheerer, M. Linseis, E. Wuttke, S. Weickert, M. Drescher, O. Tröppner, I. Ivanovic-Burmazovic, A. Irmler, F. Pauly, R. F. Winter, *Chem. Eur. J.* **2016**, *22*, 9574.
[18] P. Anders, M. Rapp, M. Linseis, R. Winter, *Inorganics* **2018**, *6*, 73.
[19] D. Fink, B. Weibert, R. F. Winter, *Chem. Commun.* **2016**, *52*, 6103.
[20] D. Fink, M. Bodensteiner, M. Linseis, R. F. Winter, *Chem. Eur. J.* **2018**, *24*, 992.
[21] D. Fink, M. Linseis, R. F. Winter, *Organometallics* **2018**, *37*, 1817.
[22] U. Pfaff, A. Hildebrandt, M. Korb, S. Osswald, M. Linseis, K. Schreiter, S. Spange, R. F. Winter, H. Lang, *Chem. Eur. J.* **2016**, *22*, 783.
[23] a) A. Karmakar, A. Paul, A. J. L. Pombeiro, *CrystEngComm* **2017**, *19*, 4666; b) J.-P. Zhang, X.-C. Huang, X.-M. Chen, *Chem. Soc. Rev.* **2009**, *38*, 2385.
[24] D. Fink, N. Orth, M. Linseis, I. Ivanović-Burmazović, R. F. Winter, *Chem. Commun.* **2020**, *56*, 1062.
[25] a) F. Pevny, R. F. Winter, B. Sarkar, S. Záliš, *Dalton Trans.* **2010**, 8000; b) E. Wuttke, Y.-M. Hervault, W. Polit, M. Linseis, P. Erler, S. Rigaut, R. F. Winter, *Organometallics* **2014**, *33*, 4672.
[26] Y.-R. Zheng, P. J. Stang, *J. Am. Chem. Soc.* **2009**, *131*, 3487.
[27] a) S. Neogi, Y. Lorenz, M. Engeser, D. Samanta, M. Schmittel, *Inorg. Chem.* **2013**, *52*, 6975; b) J.-R. Li, H.-C. Zhou, *Nat. Chem.* **2010**, *2*, 893.
[28] A. Garci, S. Marti, S. Schürch, B. Therrien, *RSC Adv* **2014**, *4*, 8597.
[29] C. Maeda, T. Yoneda, N. Aratani, M.-C. Yoon, J. M. Lim, D. Kim, N. Yoshioka, A. Osuka, *Angew. Chem. Int. Ed.* **2011**, *50*, 5691.
[30] C. Hassenrück, A. Mang, R. F. Winter, *Inorg. Chem.* **2019**, *58*, 2695.
[31] a) J. Maurer, B. Sarkar, B. Schwederski, W. Kaim, R. F. Winter, S. Záliš, *Organometallics* **2006**, 3701; b) S. Záliš, R. F. Winter, W. Kaim, *Coord. Chem. Rev.* **2010**, *254*, 1383.
[32] N. Rotthowe, J. Zwicker, R. F. Winter, *Organometallics* **2019**, *38*, 2782.
[33] A. A. Ovchinnikov, *Theor. Chim. Acta* **1978**, *47*, 297.
[34] Z. Mucsi, B. Viskolcz, I. G. Csizmadia, *J. Phys. Chem. A* **2007**, *111*, 1123.
[35] a) A. J. Churchard, M. Derzsi, Z. Jagličić, A. Remhof, W. Grochala, *Dalton Trans.* **2012**, *41*, 5172; b) A. Ishii, S. Asami, Y. Fujiwara, A. Ono, N. Nakata, *Heteroat. Chem.* **2011**, *22*, 388; c) N. R. Brooks, A. J. Blake, N. R. Champness, P. A. Cooke, P. Hubberstey, D. M. Proserpio, C. Wilson, M. Schröder, *J. Chem. Soc., Dalton Trans.* **2001**, 456; d) M. A. Watzky, D. Waknine, M. J. Heeg, J. F. Endicott, L. A. Ochrymowyzc, *Inorg. Chem.* **1993**, 4882; e) V. B. Pett, L. L. Diaddario, E. R. Dockal, P. W. Corfield, C. Ceccarelli, M. D. Glick, L. A. Ochrymowycz, D. B. Rorabacher, *Inorg. Chem.* **1983**, 3661.

Received: April 22, 2020